Electronic structure of zinc-blende MnTe investigated by photoemission and inverse-photoemission spectroscopies

Hitoshi Sato, Masaki Taniguchi, Kojiro Mimura,* Shinya Senba, and Hirofumi Namatame†
Department of Physical Sciences, Faculty of Science, Hiroshima University, Kagamiyama 1-3-1, Higashi-Hiroshima 739-8526, Japan

Yoshifumi Ueda
Kure National College of Technology, Agaminami 2-2-11, Kure 737-8506, Japan
(Received 22 October 1999)

Valence-band and conduction-band electronic structure of zinc-blende MnTe (111) epitaxial film has been investigated by ultraviolet photoemission and inverse-photoemission spectroscopies (UPS and IPES). The UPS and IPES spectra exhibit peak structures at -1.5, -3.4, and -4.3 eV, and at 3.5 and 6.7 eV relative to the valence-band maximum, respectively. Based on a one-electron band-structure calculation, peaks at -3.4 and 3.5 eV are assigned to emissions from the occupied Mn $3d\uparrow$ and unoccupied Mn $3d\downarrow$ states with nearly localized character. From their energy positions, a Mn $3d$ exchange splitting energy is estimated to be 6.9 ± 0.2 eV, which is close to that of $Cd_{1-x}Mn_xTe$ (7.0 ± 0.2 eV) and is slightly larger than that of NiAs-type MnTe (6.6 ± 0.2 eV).

I. INTRODUCTION

A stable phase of MnTe is a hexagonal NiAs-type structure below 1040 °C.[1] The cubic zinc-blende (ZB)-MnTe had been considered to be only a hypothetical compound. In 1989, Durbin *et al.*[2] succeeded in a growth of ZB-MnTe single crystal film and the quantum well by molecular-beam epitaxy (MBE). Anno, Koyanagi, and Matsubara[3] applied an ionized cluster beam deposition technique[4] to grow ZB-MnTe film. Several magnetic and optical measurements such as the magnetic susceptibility and optical absorption[3,5–7] have been performed for ZB-MnTe.

Recently, II-VI diluted magnetic semiconductors (DMS's) have attracted considerable attention as new-type semiconductors.[8–10] The DMS's are mixed crystals whose lattice is made up in part of substitutional magnetic ions. One of the most extensively studied and most thoroughly understood materials of this type is a $Cd_{1-x}Mn_xTe$ mixed crystal with ZB-type structure. In the alloy, a fraction of the Cd sublattice of CdTe is replaced by Mn atoms randomly with the Mn concentration of x up to 0.77. The distribution of the Mn ions over the cation sublattice leads to the magnetic and magneto-optical phenomena such as giant Faraday rotation. These phenomena stem from the sp-band–Mn $3d$, and Mn-Mn exchange interactions through the hybridization between the sp-band and Mn $3d$ states.

ZB-MnTe is an endpoint material of $Cd_{1-x}Mn_xTe$. For example, with increasing x, a lattice constant d of $Cd_{1-x}Mn_xTe$ decreases while its energy gap E_g increases, and they obey the virtual crystal approximation.[8] Rough extrapolations of the experimental data of d and E_g as a function of x to the $x=1$ limit provide 6.30 Å and 3.1 eV, which are close to the data of 6.34 Å and 2.92 eV for ZB-MnTe.[3] Similar extrapolation for $Zn_{1-x}Te$ also gives similar values. Accordingly, knowledge of the electronic structure of ZB-MnTe plays an important role in understanding the magnetic and magneto-optical phenomena taking place in $Cd_{1-x}Mn_xTe$.

A Mn $3d$-derived partial density of states (DOS) in the valence bands of ZB-MnTe epitaxial film grown on CdTe (100) by MBE has been obtained by resonant photoemission experiments in the Mn $3p$-$3d$ excitation region using synchrotron radiation.[11] The Mn $3d$ DOS is similar to those of $Cd_{1-x}Mn_xTe$ (Refs. 12–14) and $Zn_{1-x}Mn_xTe$ (Ref. 15) with respect to three structures at $0\sim -2.5, \sim -3.5$, and around -8 eV relative to the valence-band maximum (VBM). On the other hand, there has been no information on the conduction-band electronic structure of ZB-MnTe so far.

In this paper, we present the valence-band and conduction-band spectra of ZB-MnTe (111) epitaxial film grown onto a GaAs (100) substrate, by means of *in situ* ultraviolet photoemission and inverse-photoemission spectroscopies (UPS and IPES). We attribute the prominent structures at -3.4 and 3.5 eV relative to the VBM, to emissions from the occupied Mn $3d\uparrow$ and unoccupied Mn $3d\downarrow$ states with nearly localized character. A Mn $3d$ exchange splitting energy ($U_{\rm eff}$), which is defined as the energy necessary to add one $3d$ electron to a Mn^{2+} ion,[16,17] is estimated to be 6.9 ± 0.2 eV. The $U_{\rm eff}$ value of ZB-MnTe is similar to that of $Cd_{1-x}Mn_xTe$ (7.0 ± 0.2 eV),[18] and slightly larger than 6.6 ± 0.2 eV of NiAs-type MnTe.[19,20]

II. EXPERIMENT

The apparatus used for the present UPS and IPES experiments is composed of three ultrahigh vacuum chambers; a sample preparation chamber, an UPS chamber, and an IPES chamber. These three chambers are connected through gate valves and their base pressures are 1×10^{-10}, 7×10^{-10}, and 5×10^{-10} Torr, respectively. A schematic illustration of the present experiments is presented in Fig. 1 of Ref. 21.

The UPS spectrometer is made up of a He discharge lamp ($h\nu=21.2$ and 40.8 eV) and a double-stage cylindrical-

mirror analyzer (DCMA) to measure angle-integrated spectra. A kinetic energy of photoelectrons passing through the DCMA was fixed at 16.0 eV and its corresponding energy resolution was 0.2 eV. Under operating the He discharge lamp, the pressure of the UPS chamber was 3×10^{-9} Torr.

The IPES spectra were measured using a combination of a low-energy electron gun of Erdmann–Zipf type with a BaO cathode and a band-pass-type photon detector.[22,23] The thermal energy spread of the electron gun is 0.25 eV. Light emitted from the samples is reflected by an Al mirror coated with a MgF_2 film and focused onto the first dynode covered by a 1000-Å thick KC1 film, after passing through a SrF_2 entrance window. The maximum response of the photon detector is centered at 9.43 eV with a full width at half maximum (FWHM) of 0.47 eV. The total energy resolution of the IPES spectrometer is 0.56 eV. The electron beam was injected normal to sample surface. The UPS and IPES spectra were *in situ* measured at room temperautre, and connected at the Fermi level (E_F).

The sample used for the present experiments was ZB-MnTe (111) epitaxial film grown onto Si-doped *n*-type GaAs (100) wafer with misorientation of 2° toward the next [110] direction. The impurity concentration of the substrate is $(1.0–2.5)\times10^{18}$ cm^{-3} and its resistivity is $(1.5–2.8)\times10^{-3}$ Ω cm. Prior to the sample growth, the substrate was chemically etched in a 5:1:1 solution of $H_2SO_4:H_2O_2:H_2O$.

The sample growth was performed using a modified hot wall epitaxy (HWE) system. Polycrystalline NiAs-type MnTe, which was prepared by quenching an equal amount of Mn and Te elements in an evacuated quartz ampoule from 1000 °C to room temperature, was put into the furnace as a source material. All components of the HWE system are mounted in an ultrahigh vacuum chamber with a base pressure of 3×10^{-9} Torr and the HWE chamber is connected to the sample preparation chamber through a gate valve. A schematic illustration of the HWE system is also shown in Fig. 2 of Ref. 21.

First, the GaAs (100) substrate was heated at 600 °C for 30 min to remove the oxide layer. After the preheating process, the temperature of the substrate was decreased and was kept at 250–320 °C during the growth. The furnace with NiAs-type MnTe was operated at 860 °C and the source material was evaporated in the range of around 0.3 Å /s. After the growth, the sample was immediately transferred into the analysis chambers for UPS and IPES. In this way, a clean surface of the ZB-MnTe epitaxial film was successfully obtained.

It is well known that ZB-MnTe epitaxial films with (100) or (111) orientations grow on the GaAs (100) substrates depending on the growth condtion.[24,25] The crystal structure and (111) orientation were confirmed by x-ray diffraction for the thick films of around 3000 Å . No other phase such as NiAs-type crystal structure was detected. To avoid an electrostatic charging effect in the UPS and, in particular, IPES measurements, we reduced the film thickness until the IPES spectrum exhibited no charging effect. The (111) orientation was also confirmed by low-energy electron-diffraction (LEED) just before starting the UPS and IPES measurements. The typical thickness value of the film was around 100 Å .

The obtained UPS spectrum at $h\nu=40.8$ eV is consistent with the spectra measured near the Mn $3p$-$3d$ absorption region (~50 eV) of ZB-MnTe film, which was prepared by MBE and characterized by Auger electron spectroscopy.[11] Therefore the composition of the grown film in the present experiments is expected to be close to 1:1 in Mn:Te within the characterizations by x-ray diffraction and LEED, and we believe that the slight deviation does not change the spectral features essentially. The features of the UPS and IPES spectra including the peak structures are clearly observed as shown below, and the features were unchanged during the experiments. These results show that the present spectra are free from contamination of the sample surface.

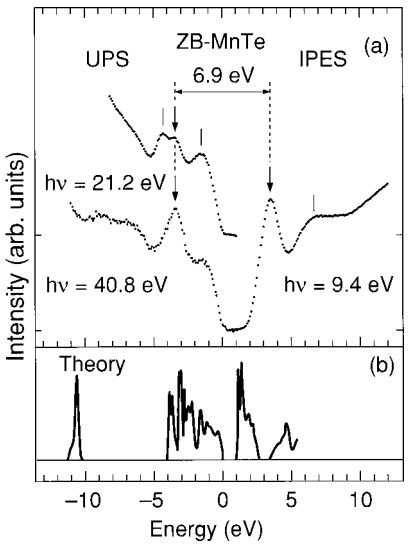

FIG. 1. (a) The UPS spectra measured at $h\nu=21.2$ and 40.8 eV and IPES spectrum of ZB-MnTe. Energy is referred to the VBM. The Mn $3d\uparrow$ and $3d\downarrow$ states will nearly localized character are observed at −3.5 and 3.4 eV, respectively. (b) The theoretical total DOS derived from the band-structure calculation (Ref. 26).

III. RESULTS AND DISCUSSION

Figure 1(a) shows the valence-band UPS spectra measured at $h\nu=21.2$ and 40.8 eV and conduction-band IPES spectrum of ZB-MnTe. The energy is referred to the VBM determined by extrapolating the steep leading edge of the highest valence-band peak to the baseline.

The UPS spectrum at $h\nu=21.2$ eV shows the structures at −1.5, −3.4, and −4.3 eV, while the spectrum at $h\nu=40.8$ eV exhibits the prominent peak at −3.4 eV with a FWHM of 1.3 eV. Two broad structures at 0~−2.5 and around −8 eV are also observed. On the other hand, the IPES spectrum shows a prominent peak at 3.5 eV with a FWHM of 1.1 eV and a broad structure around 6.7 eV. The energy separation between the prominent peaks in the UPS and IPES spectra are estimated to be 6.9 ± 0.2 eV.

Figure 1(b) shows the total DOS of ZB-MnTe derived from spin-polarized, self-consistent local-spin density total-energy band-structure calculations by Wei and Zunger.[26] Here, to the best of our knowledge, the first kind of antiferromagnetic order is assumed as the magnetic phase of ZB-MnTe (see Fig. 13 in Ref. 26). In the theoretical result, the p-d hybridization bands spread over the top 4 eV region in the valence bands and the DOS located around −11 eV

comes from the Te 5*s* states. A high DOS just above the conduction-band minimum is dominantly due to the unoccupied Mn $3d\downarrow$ states. From centers of gravity of the occupied Mn $3d\uparrow$ and unoccupied Mn $3d\downarrow$ bands, the $U_{\rm eff}$ value is estimated to be 4.7 eV.[26]

The whole feature of the theoretical DOS is in qualitative agreement with the experimental spectrum except for the broad structure around -8 eV in the UPS spectrum at $h\nu = 40.8$ eV. It is also noted that the conduction band DOS is located at a considerably lower energy side compared with the experimental spectrum.

The photoionization cross sections of the Mn 3*d* and Te 5*p* states are almost equal at $h\nu = 21.2$ eV, and the ratio (Mn 3*d*/Te5*p*) is ~ 1.1.[27] The UPS spectrum at $h\nu = 21.2$ eV, thus provides information on the Te 5*p* states as well as the Mn 3*d* states. As seen from Fig. 1(a), we find the *p*-*d* hybridization bands spread over the top 5.2 eV region in the valence bands, which is wider in comparison with 4 eV derived from the band-structure calculation.

The UPS spectrum of CdTe at $h\nu = 21.2$ eV exhibits structures at -1.5 and -4.4 eV (Ref. 18) and the two structures are assigned to maxima in the DOS of valence bands derived mainly from flat regions around the *X* and *L* symmetry points.[28,29] Assuming the band structures of the *sp*-band states in II-VI and $\mathrm{II}_{1-x}\mathrm{Mn}_x\mathrm{VI}$ semiconductors are almost common to the compounds as the first-order approximation,[8,30] the structures at -1.5 and -4.4 eV in the UPS spectrum of ZB-MnTe are also ascribed to come from flat regions around these symmetry points.

On the other hand, the photoionization cross section of the Mn 3*d* states is much larger than that of the Te 5*p* states at $h\nu = 40.8$ eV (Mn 3*d*/Te $5p = \sim 15.4$).[27] The UPS spectrum at $h\nu = 40.8$ eV thus can be regarded as coming mainly from the Mn 3*d* states. In fact, the feature of the spectrum is very similar to that of the resonant photoemission spectrum in the Mn $3p$-$3d$ excitation region using synchrotron radiation,[11] where the spectrum provides information selectively on the Mn 3*d* states. The prominent peak at -3.4 eV is attributed to the nearly localized Mn $3d\uparrow$ states. The broad structure around -8 eV, which cannot be explained by the band-structure calculation, is also related to the Mn 3*d* states. This structure shows up due to the electron-electron correlation effect as described below.

As concerns the conduction bands the prominent peak at 3.5 eV in the IPES spectrum is attributed to the Mn $3d\downarrow$ states with nearly localized character, based on the band-structure calculation.[26] The band-structure calculations by Podgórny[31] also support this assignment. The theoretical DOS corresponding to the broad structure at 6.7 eV is not shown in Refs. 26 and 31. The broad structure is assumed to be due to the higher-lying Mn 4*p*, Te 5*d*, and Te 6*s* states. The IPES spectra of CdTe (Ref. 18) and ZnTe (Ref. 21) also show the structures around 6.4 and 6.7 eV, respectively, and are attributed to the DOS features around the L and Λ symmetry points in comparison with the theoretical DOS's.[32–34] The broad structure at 6.7 eV in the IPES spectrum of ZB-MnTe would also be ascribed to come from flat regions around these symmetry points.

From the energy positions of the prominent peaks at -3.4 and 3.5 eV attributed to the Mn $3d\uparrow$ and Mn $3d\downarrow$ states, respectively, the $U_{\rm eff}$ value is estimated to be 6.9 ± 0.2 eV. Here it should again be emphasized that *in situ* measurements of the UPS and IPES spectra realize a connection of these spectra at E_F in the band gap of ZB-MnTe and make it possible to estimate the accurate $U_{\rm eff}$ value experimentally. The experimental result is considerably larger than the theoretical result of 4.7 eV, which shows that the electron-electron correlation effect is essentially important for ZB-MnTe like the other 3*d* transition-metal compounds.

Recently, we have measured the UPS spectra at $h\nu = 21.2$ eV and IPES spectra of $\mathrm{Cd}_{1-x}\mathrm{Mn}_x\mathrm{Te}$ ($0 \leqslant x \leqslant 0.7$) (Ref. 18) and $\mathrm{Zn}_{1-x}\mathrm{Mn}_x\mathrm{Te}$ ($0 \leqslant x \leqslant 0.7$) (Ref. 21) films. The UPS spectra of $\mathrm{Cd}_{1-x}\mathrm{Mn}_x\mathrm{Te}$ exhibit the structure due to the occupied Mn $3d\uparrow$ states at -3.4 eV with respect to the VBM. On the other hand, with increasing *x*, the spectral rise at the threshold and the width of the first peak in the IPES spectra become steep and narrow, respectively, while the energy of the first peak remains almost unchanged at 3.6 eV. In addition, the first peak is assumed to exhibit a slight increase in intensity with *x*.

With these results, we have assigned the peak at 3.6 eV to the Mn $3d\downarrow$ states and estimated the $U_{\rm eff}$ value to be 7.0 eV. The band-structure calculations for CdTe and $\mathrm{Cd}_{0.4}\mathrm{Mn}_{0.6}\mathrm{Te}$ (Ref. 16) also show that the contribution of the Mn $3d\downarrow$ states shows up just at the first DOS peak of CdTe. The present experimental results of ZB-MnTe support our previous assignment of the first peak in the IPES spectra of $\mathrm{Cd}_{1-x}\mathrm{Mn}_x\mathrm{Te}$ to the unoccupied Mn $3d\downarrow$ states and the $U_{\rm eff}$ value of 7.0 eV.

In the case of $\mathrm{Zn}_{1-x}\mathrm{Mn}_x\mathrm{Te}$ ($0 \leqslant x \leqslant 0.7$), the structure due to the occupied Mn $3d\uparrow$ states is observed at -3.7 eV in the UPS spectra.[21] On the other hand, with increasing *x* up to 0.3, the unoccupied Mn $3d\downarrow$ states appear as a shoulder at the lower energy side of the first peak at 4.0 eV in the IPES spectrum of ZnTe. At and above $x = 0.6$, the spectral shape of the first peak becomes a clear single peak at 3.5 eV. Then, the energy position of the Mn $3d\downarrow$ states was estimated to be 3.5 eV by taking directly the peak position, and the $U_{\rm eff}$ value of $\mathrm{Zn}_{1-x}\mathrm{Mn}_x\mathrm{Te}$ was derived to be 7.2 ± 0.2 eV.[21]

Previously, we paid little attention to the difference between the $U_{\rm eff}$ values of 7.0 eV for $\mathrm{Cd}_{1-x}\mathrm{Mn}_x\mathrm{Te}$ and 7.2 eV for $\mathrm{Zn}_{1-x}\mathrm{Mn}_x\mathrm{Te}$, and regarded them as almost the same values within the experimental accuracy. Our view of the $U_{\rm eff}$ values was consistent with the result of the local coordination around a Mn atom in $\mathrm{Cd}_{1-x}\mathrm{Mn}_x\mathrm{Te}$ and $\mathrm{Zn}_{1-x}\mathrm{Mn}_x\mathrm{Te}$ obtained by means of the extended x-ray absorption fine-structure (EXAFS) spectroscopy.[35,36] The EXAFS experiments revealed that a MnTe_4 tetrahedron is embedded in these alloys with a well-preserved form and the Mn-Te distance and the bond angle of the MnTe_4 cluster are almost independent of *x*.

The present experiments for ZB-MnTe show that its $U_{\rm eff}$ value is 6.9 eV and only the $U_{\rm eff}$ value of $\mathrm{Zn}_{1-x}\mathrm{Mn}_x\mathrm{Te}$ is slightly larger among those of $\mathrm{Cd}_{1-x}\mathrm{Mn}_x\mathrm{Te}$, $\mathrm{Zn}_{1-x}\mathrm{Mn}_x\mathrm{Te}$, and ZB-MnTe. The Mn-Te distance and the bond angle of the MnTe_4 cluster in $\mathrm{Cd}_{1-x}\mathrm{Mn}_x\mathrm{Te}$ (Ref. 35) and $\mathrm{Zn}_{1-x}\mathrm{Mn}_x\mathrm{Te}$ (Ref. 36) are, on the other hand, almost the same as those of ZB-MnTe.[3] These facts bring up a possibility of the smaller $U_{\rm eff}$ value for $\mathrm{Zn}_{1-x}\mathrm{Mn}_x\mathrm{Te}$, passed unnoticed so far; the structure due to the Mn $3d\downarrow$ states in the IPES spectra of $\mathrm{Zn}_{1-x}\mathrm{Mn}_x\mathrm{Te}$ is actually at a lower energy

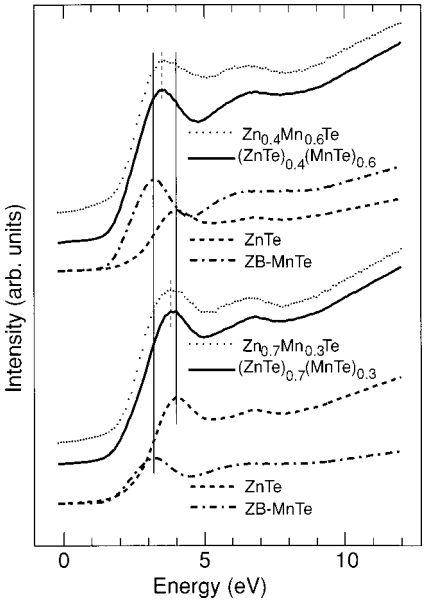

FIG. 2. Comparison between the IPES spectra of $Zn_{1-x}Mn_xTe$ for $x=0.3$ and 0.6 (Ref. 21, dotted curves) and the spectra constructed using those of ZnTe (Ref. 21) and ZB-MnTe with molar ratios (solid curves). The IPES spectra of $Zn_{1-x}Mn_xTe$ (Ref. 21) are comparatively well reproduced by the constructed spectra. The IPES spectra of ZnTe and ZB-MnTe are also shown.

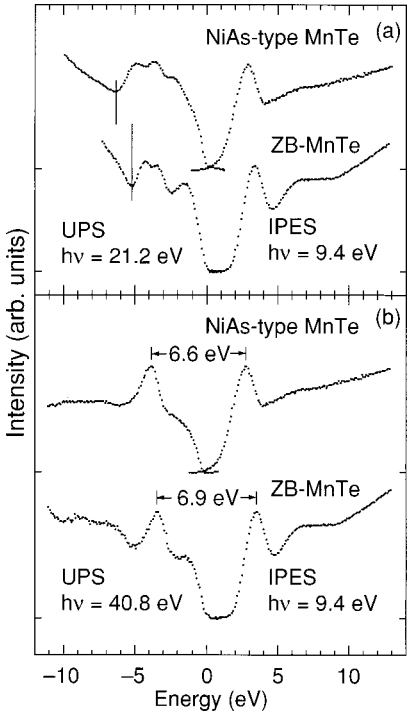

FIG. 3. The UPS spectra measured at $h\nu=21.2$ and 40.8 eV and IPES spectrum of NiAs-type MnTe (Refs. 19 and 20) together with those of ZB-MnTe. Energy is referred to the VBM. The U_{eff} value is smaller and the bandwidth of the p-d hybridization band is wider in NiAs-type MnTe. The differences of each spectra are summarized in Table I.

than 3.5 eV, though the peak looks experimentally at 3.5 eV, lower energy by 0.5 eV than the first peak in the IPES spectrum of ZnTe.

To examine the possibility, we compare the IPES spectra of $Zn_{1-x}Mn_xTe$ (Ref. 21) with the spectra constructed using those of ZnTe (Ref. 21) and ZB-MnTe in Fig. 2. Before the construction, we tentatively place the first peak of ZB-MnTe at 3.2 eV, assuming that the U_{eff} value of $Zn_{1-x}Mn_xTe$ is 6.9 ev, and normalize the intensities of the first peaks of ZnTe and ZB-MnTe to unity.

The first peaks in the IPES spectra of ZnTe and ZB-MnTe are composed of the sp-band states, the Mn $3d$ states, and the background due to incident electrons scattered inelastically before emitting photons. To evaluate the ratio of the inverse-photoemission intensities for the first peaks, information on the cross sections of each state and contribution of the background is required. However, it is generally difficult at present. In particular, the method to deduce the background of the IPES spectra has not been established, although attempts using electron-energy-loss spectra have been carried out.[37]

In the present paper, for simplicity, we have constructed the IPES spectra of $Zn_{1-x}Mn_xTe$ using those of ZnTe and ZB-MnTe with just the molar ratio. The results are shown in Fig. 2 by solid curves together with the IPES spectra of ZnTe and ZB-MnTe. It should be noticed that the spectra constructed with just the molar ratios (ZnTe/ZB-MnTe) of 0.3/0.7 and 0.6/0.4, comparatively well reproduce the features, in particular, peak positions of the IPES spectra of $Zn_{1-x}Mn_xTe$ with $x=0.3$ and $x=0.6$,[21] shown by dotted curves, respectively. This suggests that the inverse-photoemission intensities of the first peaks are accidentally almost the same for ZnTe and ZB-MnTe and the energy position of the Mn $3d\downarrow$ states in $Zn_{1-x}Mn_xTe$ is around 3.2 eV.

Based on the discussion above, we change our view on the previous result (Ref. 21) and again assume the U_{eff} value of $Zn_{1-x}Mn_xTe$ to be 6.9 ± 0.2 eV, which is close to those of $Cd_{1-x}Mn_xTe$ and ZB-MnTe. The present results for ZB-MnTe provide us with the unified picture for the electronic structure of the $Cd_{1-x}Mn_xTe$, $Zn_{1-x}Mn_xTe$, and ZB-MnTe. To derive the more accurate energy position of the Mn $3d\downarrow$ states of $Zn_{1-x}Mn_xTe$, the resonant IPES experiments in the Mn $3p$-$3d$ excitation region, which provide information selectively on the unoccupied Mn $3d\downarrow$ states, are required.

Next we compare the UPS and IPES spectra of ZB-MnTe with those of NiAs-type MnTe.[19,20] Figure 3(a) shows the UPS spectrum at $h\nu=21.2$ eV and IPES spectrum of NiAs-type MnTe (Refs. 19 and 20) together with those of ZB-MnTe. The energy is referred to the VBM of the respective samples. The UPS spectrum at $h\nu=21.2$ eV of NiAs-type MnTe shows three structures at -2.4, -3.8, and -5.0 eV, and the p-d hybridization bands spread over the top 6.5 eV region in the valence bands, which is wider than 5.2 eV of ZB-MnTe. The IPES spectrum of NiAs-type MnTe exhibits a prominent peak at 2.9 eV and a broad structure around 6.5 eV.

The UPS spectra at $h\nu=40.8$ eV and again the IPES spectra of both phases are compared in Fig. 3(b). The whole feature of their spectra is similar. The prominent peaks at -3.7 and 2.9 eV of NiAs-type MnTe are due to the occupied Mn $3d\uparrow$ and unoccupied Mn $3d\downarrow$ states with nearly localized character, respectively. This provides the U_{eff} value of

TABLE I. Experimental results of ZB-MnTe and NiAs-type MnTe (Refs. 19 and 20). U_{eff}, Mn $3d$ exchange splitting energy; $W_{p\text{-}d}$, bandwidth of UPS spectrum at $h\nu=21.2$ eV; $E_{3d\uparrow}$, energy position of main peak in UPS spectrum at $h\nu=40.8$ eV; $E_{3d\downarrow}$, energy position of main peak in IPES spectrum. All values are in eV units. The bond lengths are also shown in Å units as R.

	ZB-MnTe	NiAs-type MnTe
Symmetry	Cubic	Hexagonal
U_{eff}	6.9	6.6
$W_{p\text{-}d}$	5.2	6.5
$E_{3d\uparrow}$	-3.4	-3.7
$E_{3d\downarrow}$	3.5	2.9
R[Mn-Te]	2.74	2.92
R[Mn-Mn]	4.47	3.36
R[Te-Te]	4.47	4.12

6.6 eV, which is slightly smaller than 6.9 eV of ZB-MnTe. The broad structure around -8 eV is also observed in the UPS spectrum at $h\nu=40.8$ eV of NiAs-type MnTe.

The Mn-Te distances in NiAs-type MnTe and ZB-MnTe are 2.92 and 2.74 Å , respectively (see Table I). Taking into account only the Mn-Te distance, the degree of the p-d hybridization of NiAs-type MnTe should be lower than that of ZB-MnTe and therefore its bandwidth of the p-d hybridization band is expected to be narrower, which is in contradiction to the present experimental result. However, as pointed out by Podgórny,[31] it is important to take into account also the Mn-Mn and Te-Te distances in both phases for a comparison. They are 3.36 and 4.12 Å in NiAs-type MnTe and 4.47 and 4.47 Å in ZB-MnTe, respectively (see Table I). Much smaller values of the Mn-Mn and Te-Te distances in NiAs-type MnTe cause a wider Mn $3d$–Te $5p$ bandwidth in comparison with ZB-MnTe. Furthermore, an atomic volume of ZB-MnTe is also larger by $\sim$27% than NiAs-type MnTe and we expect a denser system to exhibit more delocalized states.[31]

The p-d bandwidths for both phases are, thus, explained by taking into account the distances of the second nearest neighbor and the atomic volume. The smaller U_{eff} value of NiAs-type MnTe is also described from the viewpoint of the more delocalized Mn $3d$ states due to the shorter Mn-Mn distance, and this leads to the weaker Mn $3d$-$3d$ Coulomb interaction with the Mn atom.

The differences between ZB- and NiAs-type MnTe such as the p-d bandwidth, the U_{eff} value, and energy positions of the occupied Mn $3d\uparrow$ and unoccupied Mn $3d\downarrow$ states relative to the VBM are qualititvely reproduced by the band-structure calculations.[26] The experimental results for both phases as well as the interatomic distances are summarized in Table I.

Finally, we comment on the broad structure around -8 eV in the UPS spectrum of ZB-MnTe measured at $h\nu=40.8$ eV. This structure cannot be explained by the band-structure calculations based on the one-electron picture. The whole feature of the Mn $3d$ partial DOS of ZB-MnTe (Ref. 11) is similar to those of $Cd_{1-x}Mn_xTe$ (Refs. 12–14) and $Zn_{1-x}Mn_xTe$ (Ref. 15) with respect to three characteristic structures: valence bands at $0\sim-2.5$ eV, a main peak at ~-3.5 eV, and a satellite structure around -8 eV. The Mn $3d$ spectrum has been explained by a configuration interaction (CI) theory with a multielectron picture.[38,39] In comparison with the CI theory applied to the Mn $3d$ spectrum of $Cd_{1-x}Mn_xTe$,[13,39] the satellite structure around -8 eV is attributed to transition into d^4 final states. On the other hand, the structure at $0\sim-5$ including the main peak is assigned to $d^5\underline{L}$ final states, where $\underline{L}$ represents a ligand hole.[40]

IV. SUMMARY

The valence-band and conduction-band electronic structure of ZB-MnTe (111) epitaxial film grown on the GaAs (100) substrate has been investigated by *in situ* measurements of the UPS and IPES spectra. On the basis of the one-electron band-theory,[28,29,32–34] peaks structures at -4.3, -1.5, and 6.7 eV are ascribed to the DOS maxima derived mainly from the flat regions around the X, L, and L and Λ symmetry points, respectively, assuming common features in II-VI and $II_{1-x}Mn_xVI$ compounds as the first-order approximation.[8] In addition, the prominent peaks at -3.4 and 3.5 eV are attributed to the occupied Mn $3d\uparrow$ and unoccupied $3d\downarrow$ states with nearly localized character, respectively, and the U_{eff} value is derived to be 6.9 ± 0.2 eV.

The whole feature of the UPS and IPES spectra of ZB-MnTe is similar to that of $Cd_{1-x}Mn_xTe$, and the U_{eff} value of ZB-MnTe is also close to 7.0 eV of $Cd_{1-x}Mn_xTe$.[18] Comparison of the IPES spectra of $Zn_{1-x}Mn_xTe$ (Ref. 21) with the spectra constructed using those of ZnTe (Ref. 21) and ZB-MnTe, led us to change the previous estimation for the U_{eff} value of $Zn_{1-x}Mn_xTe$ and again assume it to be 6.9 eV. The present results for ZB-MnTe provide us the unified picture for the electronic structure of the $Cd_{1-x}Mn_xTe$, $Zn_{1-x}Mn_xTe$, and ZB-MnTe.

On the other hand, the U_{eff} value and the bandwidth of the p-d hybridization band of ZB-MnTe is slightly larger and narrower in comparison with those of NiAs-type MnTe,[19,20] respectively. These experimental results are explained by taking into account the second nearest neighbor and the atomic volume.[31]

ACKNOWLEDGMENTS

The authors are grateful to Professor K. Ando for providing us information on the sample preparation, to J. Harada and K. Miyazaki for their assistance in the sample preparation, and to Y. Kani for the data analysis. This work was supported by the Grant-in-Aid for Scientific Research from the Ministry of Education, Science and Culture, Japan.

*Present address: Department of Mathematical Science, College of Engineering, Osaka Prefecture University, Gakuen 1-1, Sakai, Osaka 559-8531, Japan.

†Present address: Hiroshima Synchrotron Radiation Center, Hiroshima University, Kagamiyama 2-313, Higashi-Hiroshima 739-8526, Japan.

[1] W. D. Johnston and A. E. Sestrich, J. Inorg. Nucl. Chem. **19**, 229 (1961).

[2] S. M. Durbin, J. Han, O. Sungki, M. Kobayashi, D. R. Menke, R. L. Gunshor, Q. Fu, N. Pelekanos, A. V. Nurmikko, D. Li, J. Gonsalves, and N. Otsuka, Appl. Phys. Lett. **55**, 2087 (1989).
[3] H. Anno, T. Koyanagi, and K. Matsubara, J. Cryst. Growth **117**, 816 (1992).
[4] T. Koyanagi, K. Matsubara, H. Takaoka, and T. Takagi, J. Appl. Phys. **61**, 3020 (1987).
[5] K. Ando, K. Takahashi, and T. Okuda, J. Magn. Magn. Mater. **104-107**, 993 (1992).
[6] K. Ando K. Takahashi T. Okuda, and M. Umehara, Phys. Rev. B **46**, 12289 (1992).
[7] K. Ando, Phys. Rev. B **47**, 9350 (1993).
[8] J. K. Furdyna, J. Appl. Phys. **64**, R29 (1988).
[9] *Diluted Magnetic Semiconductors*, edited by J. K. Furdyna and J. Kossut, Semiconductors and Semimetals Vol. 25 (Academic, New York, 1988), and references therein.
[10] *Diluted Magnetic Semiconductors*, edited by M. Jain (World Scientific, Singapore, 1991), and references therein.
[11] P. R. Bressler and H.-E. Gumlich, J. Cryst. Growth **138**, 1028 (1994).
[12] M. Taniguchi, L. Ley, R. L. Johnson, J. Ghijsen, and M. Cardona, Phys. Rev. B **33**, 1206 (1986).
[13] L. Ley, M. Taniguchi, J. Ghijsen, R. L. Johnson, and A. Fujimori, Phys. Rev. B **35**, 2839 (1987).
[14] N. Happo, H. Sato, K. Mimura, S. Hosokawa, M. Taniguchi, Y. Ueda, and M. Koyama, Phys. Rev. B **50**, 12211 (1994).
[15] M. Taniguchi, K. Soda, I. Souma, and Y. Oka, Phys. Rev. B **46**, 15789 (1992).
[16] H. Ehrenreich, K. C. Hass, N. F. Johnson, B. E. Larson, and R. J. Lampert, in *Proceedings of the 18th International Conference of the Physics of Semiconductors*, edited by O. Engstrom (World Scientific, Singapore, 1987), pp. 1751–1754.
[17] B. E. Larson, K. C. Hass, H. Ehrenreich, and A. E. Carlsson, Phys. Rev. B **37**, 4137 (1988).
[18] M. Taniguchi, K. Mimura, H. Sato, J. Harada, K. Miyazaki, H. Namatame, and Y. Ueda, Phys. Rev. B **51**, 6932 (1995).
[19] H. Sato, M. Tamura, N. Happo, T. Mihara, M. Taniguchi, T. Mizokawa, A. Fujimori, and Y. Ueda, Solid State Commun. **92**, 921 (1994).
[20] Y. Ueda, H. Sato, M. Taniguchi, N. Happo, T. Mihara, H. Namatame, T. Mizokawa, and A. Fujimori, J. Phys.: Condens. Matter **6**, 8607 (1994).
[21] M. Taniguchi, N. Happo, K. Mimura, H. Sato, J. Harada, K. Miyazaki, H. Namatame, Y. Ueda, and M. Ohashi, J. Phys.: Condens. Matter **7**, 4371 (1995).
[22] K. Yokoyama, K. Nishihara, K. Mimura, Y. Hari, M. Taniguchi, Y. Ueda, and M. Fujisawa, Rev. Sci. Instrum. **64**, 87 (1993).
[23] Y. Ueda, K. Nishihara, K. Mimura, Y. Hari, M. Taniguchi, and M. Fujisawa, Nucl. Instrum. Methods Phys. Res. A **330**, 140 (1993).
[24] H. Akinaga, K. Ando, T. Abe, and S. Yoshida, J. Appl. Phys. **74**, 746 (1993).
[25] H. Akinaga and K. Ando, Appl. Surf. Sci. **75**, 292 (1994).
[26] S.-H. Wei and A. Zunger, Phys. Rev. B **35**, 2340 (1987).
[27] J. J. Yeh and I. Lindau, At. Data Nucl. Data Tables **32**, 45 (1985); **32**, 72 (1985).
[28] L. Ley, A. Pollak, F. R. McFeely, S. P. Kowalczyk, and D. A. Shirley, Phys. Rev. B **9**, 600 (1974).
[29] N. J. Shevchik, J. Tejeda, and M. Cardona, Phys. Rev. B **9**, 2627 (1974).
[30] The valence electrons of the Mn atom is $4s^2$ orbitals. The Mn $3d$ orbitals are exactly half-filled by Hund's rule and the $3d^5$ configurations act as a complete shell like the $3d^{10}$ shell in the Zn atom and the $4d^{10}$ shell in the Cd atom. Accordingly, this assumption would be plausible.
[31] M. Podgórny, Z. Phys. B: Condens. Matter **69**, 501 (1988).
[32] J. R. Cherikowski and M. L. Cohen, Phys. Rev. B **14**, 556 (1976).
[33] M. L. Cohen and T. K. Bergstresser, Phys. Rev. **141**, 789 (1966).
[34] S. I. Kurganskii, O. V. Farveroich, and E. P. Domashevskaya, Fiz. Tekh. Poluprovodn. **14**, 1315 (1980) [Sov. Phys. Semicond. **14**, 775 (1980)].
[35] A. Balzarotti, N. Motta, A. Kisiel, M. Zimnal-Starnawska, M. T. Czyzyk, and M. Podgórny, Phys. Rev. B **31**, 7526 (1985).
[36] N. Happo, H. Sato, T. Mihara, K. Mimura, S. Hosokawa, Y. Ueda, and M. Taniguchi, J. Phys.: Condens. Matter **8**, 4315 (1996).
[37] K. W. Goodman and V. E. Henrich, Phys. Rev. B **49**, 4827 (1994).
[38] A. Fujimori and F. Minami, Phys. Rev. B **30**, 957 (1984).
[39] T. Mizokawa and A. Fujimori, Phys. Rev. B **48**, 14 150 (1993).
[40] The Mn $3d$ DOS of ZB-MnTe (Ref. 11) is different from that of NiAs-type MnTe in relative intensities (Refs. 19 and 20). The CI analysis of the Mn $3d$ spectrum is performed with adjustable parameters; Coulomb interaction energy, p-d charge transfer energy, and p-d transfer integral. Among these parameters, the p-d transfer integral $(pd\sigma)$ is significantly important in the difference of the Mn $3d$ spectra of ZB-MnTe and NiAs-type MnTe. The $(pd\sigma)$ derived using a tetrahedral $MnTe_4$ cluster is -1.1 eV for $Cd_{1-x}Mn_xTe$ (Ref. 39), which would be close to that of ZB-MnTe, while -0.75 eV for NiAs-type MnTe (Refs. 19 and 20) with an octahedral $MnTe_6$ cluster. Transfer integrals T_{t_2} and T_e between the Mn $3d$ orbitals and the ligand (p-) molecular orbitals with t_2 and e symmetries are given by $T_{t_2}=\sqrt{4/3(pd\sigma)^2+8/9(pd\pi)^2}$ and $T_e=2\sqrt{6}/3(pd\pi)$ for a system with a tetrahedral symmetry, and $T_{t_2}=2(pd\pi)$ and $T_e=-\sqrt{3}(pd\sigma)$ with an octahedral symmetry (Ref. 39). Assuming $(pd\sigma)/(pd\pi)=-2.16$ (Ref. 39), derived $(pd\sigma)$ provide $T_{t_2}=1.4$ eV and $T_e=0.8$ eV for ZB-MnTe and $T_{t_2}=0.7$ eV and $T_e=1.2$ eV for NiAs-type MnTe. The effective p-d transfer integral averaged by degeneracy of the orbitals with t_2 and e symmetries of ZB-MnTe is 1.2 eV and greater than 0.9 eV of NiAs-type MnTe as far as only the nearest neighbors are concerned. In order to obtain more information such as the d-d transfer integral, the CI analysis using a larger cluster is required.